Stat3 regulates microtubules by antagonizing the depolymerization activity of stathmin

Dominic Chi Hiung Ng,[1] Bao Hong Lin,[1] Cheh Peng Lim,[1] Guochang Huang,[1] Tong Zhang,[1] Valeria Poli,[2] and Xinmin Cao[1]

[1]Signal Transduction Laboratory, Institute of Molecular and Cell Biology, Singapore 138673, Republic of Singapore
[2]Department of Genetics, Biology, and Biochemistry, University of Turin, 10126 Turin, Italy

Stat3 is a member of the signal transducer and activator of transcription family, which is important in cytokine signaling. Gene ablation studies have revealed a requirement for Stat3 in diverse biological processes (Akira, S. 2000. *Oncogene.* 19: 2607–2611; Levy, D.E., and C.K. Lee. 2002. *J. Clin. Invest.* 109:1143–1148). Previously, the function of Stat3 had been attributed exclusively to its transcriptional activity in the nucleus. In this study, we reveal an interaction between Stat3 and the microtubule (MT)-destabilizing protein stathmin. Stathmin did not overtly affect ligand-stimulated Stat3 activation. In contrast, the expression of Stat3 is required for the stabilization of MTs and cell migration. We further demonstrate that Stat3-containing cells are resistant to the MT-destabilizing effect of stathmin overexpression. In addition, down-regulation of stathmin protein levels in Stat3-deficient cells partially reversed the MT and migration deficiencies. Recombinant Stat3 was also capable of reversing stathmin inhibition of tubulin polymerization in vitro. Our results indicate that Stat3 modulates the MT network by binding to the COOH-terminal tubulin-interacting domain of stathmin and antagonizing its MT destabilization activity.

Introduction

The STAT (signal transducer and activator of transcription) family is comprised of seven members in mammals, of which Stat3 is the most pleiotropic member implicated in several biological processes (Levy and Lee, 2002). Specifically, it has been established as an oncogene by cell transformation and tumor formation capacities in gain-of-function studies (Bromberg et al., 1999; Bromberg, 2002). In addition, constitutive Stat3 activation has been reported in a multitude of human cancers (Bowman et al., 2000). The oncogenic potential of Stat3 was initially attributed to a positive influence on cell proliferation and/or protection from cell death (for review see Bromberg and Darnell, 2000). However, a multifunctional role for Stat3 in promoting tumor growth is emerging, with Stat3 implicated in mediating cell motility and invasiveness, nutrient supply through augmenting angiogenesis, and in masking tumors from the body's innate immune defenses (Wei et al., 2003; Silver et al., 2004; Wang et al., 2004). In addition to tumorigenesis, Stat3 knockout in mice causes early embryonic lethality (Takeda et al., 1997). Furthermore, conditional knockout mice revealed a critical role for Stat3 in migrating keratinocytes involved in wound healing of the skin (Sano et al., 1999). These studies, in addition to conditional Stat3 ablation studies in other tissues (Akira, 2000; Levy and Lee, 2002), indicate that Stat3 function extends beyond its tumorigenic potential.

Despite the wide range in function, the molecular events leading to Stat3 activation remain relatively straightforward. The canonical Stat3 activation pathway involves cytokine-induced receptor subunit multimerization and activation of receptor-associated Janus tyrosine kinases at the intracellular domain (Darnell et al., 1994). Janus tyrosine kinase phosphorylation of the receptor subunits subsequently recruits latent Stat3 from the cytoplasm via Src homology 2 domain interaction (Heim et al., 1995). In turn, Stat3 is phosphorylated, dimerizes, and nuclear translocates to regulate gene expression. Several Stat3 target genes have been identified, including cyclin D1, c-myc, Bcl-2, and Bcl-X_L (Turkson and Jove, 2000), which may be critical in Stat3-mediated tumorigenesis by regulating cell cycle and survival. However, it remains unclear how Stat3 regulates cell migration. In addition, it is unclear whether cytoplasmic Stat3, the majority of Stat3 population in normal cells, plays any role independent of its transcriptional activity.

Correspondence to Xinmin Cao: mcbcaoxm@imcb.a-star.edu.sg

T. Zhang's present address is Department of Medicine, University of California, San Diego, La Jolla, CA 92093.

Abbreviations used in this paper: ΔSt3, Stat3 deficient; GAPDH, glyceraldehyde-3-phosphate dehydrogenase; HU, hydroxyurea; IL-6, interleukin 6; MEF, murine embryonic fibroblast; MT, microtubule; SCG10, super cervical ganglion protein 10; SCLIP, SCG10-like protein; siRNA, short inhibitory RNA; SLD, stathmin-like domain; TCL, total cell lysate; WT, wild type.

The online version of this article contains supplemental material.

The Journal of Cell Biology, Vol. 172, No. 2, January 16, 2006 245–257
http://www.jcb.org/cgi/doi/10.1083/jcb.200503021

Stathmin, also known as oncoprotein 18, is a small (18 kD) ubiquitous phosphoprotein localized predominantly to the cytosol. The related stathmin-like family members include super cervical ganglion protein 10 (SCG10), SCG10-like protein (SCLIP), and RB3. These stathmin-related proteins share highly homologous tubulin-binding stathmin-like domains (SLDs) at their COOH terminus (Charbaut et al., 2001). In addition, they possess a variable membrane-anchoring NH_2-terminal region that localizes the proteins predominantly to the Golgi apparatus (Gavet et al., 1998).

Stathmin was originally identified as a key factor involved in regulating cell proliferation (Sobel et al., 1989). More recently, stathmin's ability to bind α/β-tubulin heterodimers to facilitate the depolymerization of microtubules (MTs; Belmont and Mitchison, 1996) was identified as a principle mechanism of action associated with the control of mitotic spindle assembly as well as other processes involving MT dynamics (Marklund et al., 1994; Iancu et al., 2001). Of particular relevance to this study are previous reports of the contribution of stathmin to cell motility (Baldassarre et al., 2005; Giampietro et al., 2005). However, the exact mechanism by which stathmin mediates this process remains unclear. Because of their compartmental restrictions, the functions of stathmin-like proteins are likely to be more specified compared with stathmin, although this also remains largely uncharacterized.

In this study, we present evidence of Stat3 interacting with stathmin. Moreover, our results reveal that Stat3 may modulate MT dynamics and cell migration through a direct functional interaction with stathmin in the cytoplasm.

Results

Stathmin is a Stat3-interacting protein

We initially identified SCLIP as an interacting protein of Stat3 in a yeast two-hybrid screen of a mouse brain library using the COOH-terminal portion of Stat3 (aa 395–770) as bait. The interaction between exogenously expressed proteins was subsequently confirmed in mammalian COS-1 cells (unpublished data). Next, we tested for an interaction with Stat3 among other members of the stathmin family. We observed that myc-tagged SCLIP and stathmin but not myc-SCG10 was shown to associate with endogenous Stat3 in PC12 cells (Fig. 1 A). Because the biological functions of stathmin are better characterized compared with SCLIP, we focused our study on stathmin. As a result of the high expression of stathmin in neuronal cells, the endogenous association with Stat3 was tested in PC12 and NSC34 cells. The results showed that endogenous stathmin coimmunoprecipitated with the Stat3-specific antibody but not rabbit IgG in both cell lines (Fig. 1 B). Finally, we sought to determine whether the interaction between Stat3 and stathmin was direct. GST-stathmin was expressed and purified from *Escherichia coli*, and its interaction with a baculovirus-produced His-tagged Stat3 was examined. Fig. 1 C shows that His-Stat3 (97 kD) and GST-stathmin (46 kD) are the major proteins in the Coomassie blue–stained gel. Association between His-tagged Stat3 and GST-stathmin was then determined by a pull-down assay with glutathione–Sepharose beads. In Fig. 1 D, a marginal amount of Stat3 was found associating with the GST. However, substantially greater amounts of Stat3 were pulled down by GST-stathmin. To exclude the possibility that stathmin associated with the His-tag nonspecifically, we showed that both GST alone and GST-stathmin did not interact with an irrelevant His-tagged protein, His-COMT (catechol-O-methyltransferase; Fig. 1 E). Altogether, these results demonstrate a direct physiological association of Stat3 with stathmin.

Stathmin proteins do not affect Stat3 signaling

To determine the function of Stat3 association with stathmin proteins, we first investigated the effect of modulating stathmin expression on Stat3 signaling. Overexpression of myc-stathmin or short inhibitory RNA (siRNA) down-regulation of endogenous stathmin in PC12 cells did not significantly affect Stat3 transcriptional activity stimulated by interleukin (IL)-6, as determined by a luciferase reporter assay (Fig. 2, A and B). In addition, stimulated Stat3 Y705 and S727 phosphorylation remained unchanged during overexpression (not depicted) or knockdown of stathmin protein (Fig. 2 C). Finally, we showed that stathmin overexpression did not prevent Stat3 nuclear translocation stimulated by IL-6 (Fig. 2 D). Collectively, these experiments demonstrate that stathmin does not augment or perturb ligand-stimulated Stat3 signaling in terms of phosphorylation, capacity of nuclear translocation, and promoting transcription.

Stat3-deficient (ΔSt3) MEF cells exhibit an impaired MT network

We next investigated whether an interaction with Stat3 influenced stathmin activity by first looking at the MT network in murine embryonic fibroblasts (MEFs) genetically depleted of Stat3 (Costa-Pereira et al., 2002). Staining for α-tubulin revealed radial arrays of MTs in the wild-type (WT) MEF cells (Fig. 3 A, i). Strikingly, the MT array in ΔSt3 MEFs appeared disorganized, with thin, discontinuous filaments and few MTs radiating from the centrosome to the plasma membrane (Fig. 3 A, iv). Quantitative analysis of the α-tubulin staining in randomly selected cells indicated that the fluorescence intensity in ΔSt3 MEFs (40 ± 14 intensity units/μm^2; $n = 12$) were ~40% of that in WT MEFs (94 ± 18 intensity units/ μm^2; $n = 12$; not depicted). Further analysis with anti-acetylated α-tubulin revealed dramatically reduced levels of this MT subset in ΔSt3 MEFs compared with WT cells (Fig. 3 A, ii and v). Furthermore, we compared MTs at the same cell cycle stage by arresting cells at the G_1/S transition with hydroxyurea (HU). Arresting WT MEFs with HU resulted in substantially increased acetylated MTs (Fig. 3 A, iii). In contrast, ΔSt3 cells displayed a marginal increase after HU treatment (Fig. 3 A, vi). As post-translational acetyl modification correlates with increased MT stability (Webster and Borisy, 1989), these results indicate that the ΔSt3 MEFs are deficient in stabilized long-life MTs. We further confirmed this biochemically. Initially, we examined the total expression of α-tubulin and acetylated α-tubulin in MEF cells. Densitometric quantitation of α-tubulin bands, normalized for glyceraldehyde-3-phosphate dehydrogenase (GAPDH) expression, indicated that there was not a marked difference

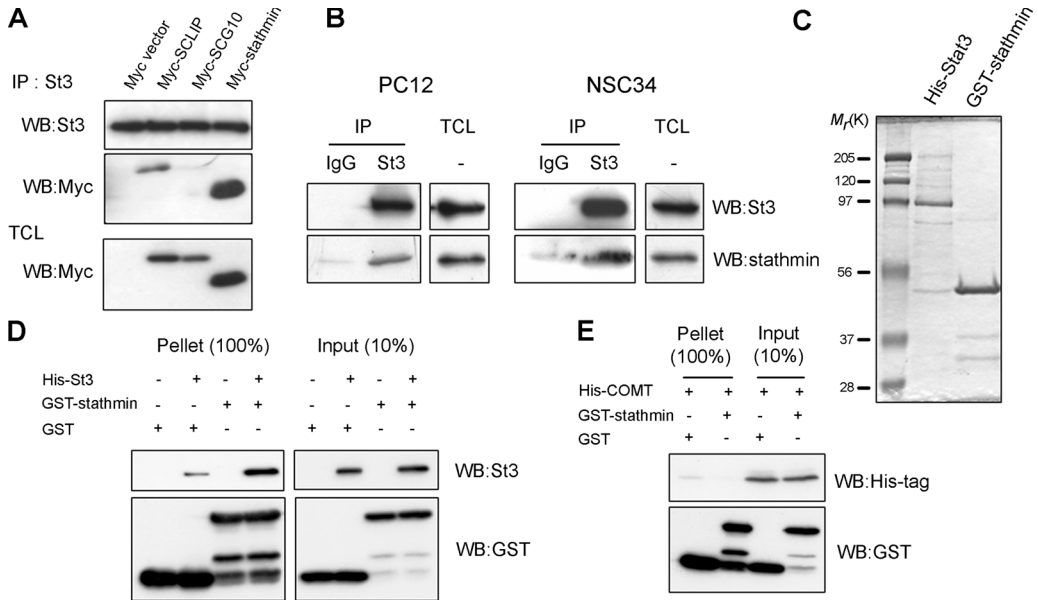

Figure 1. **Association of Stat3 with stathmin.** (A) PC12 cells were transfected with myc-tagged SCLIP, SCG10, and stathmin or vector alone. Endogenous Stat3 was immunoprecipitated, and the associated proteins were evaluated by blotting with anti-myc. The expression of myc-tagged proteins in total cell lysates (TCLs) was also determined by Western blotting. (B) Association of endogenous stathmin with Stat3 in PC12 and NSC34 cells was determined by immunoprecipitation with Stat3 antibody and blotting for stathmin. Substitution of the Stat3 antibody with a normal rabbit IgG antibody served as a control. Protein expression levels of Stat3 and stathmin in TCLs were analyzed. (C) Purified recombinant His-tagged Stat3 and GST-stathmin were Coomassie blue stained. (D) 3 μg His-tagged Stat3 and 3 μg GST-stathmin were preincubated and subjected to a GST pull-down assay. Interaction with GST-stathmin was then determined by blotting with anti-Stat3. Pull-down efficiency was shown by blotting for GST. GST alone was used as a negative control. An aliquot of each reaction before pull-down was similarly blotted to indicate protein input. (E) GST-stathmin pull-down was repeated with an irrelevant His-tagged protein (His-COMT).

between ΔSt3 and WT MEFs. In contrast, acetylated α-tubulin levels after normalizing for GAPDH expression were ~35% lower in ΔSt3 MEFs compared with WT. Stat3 was also confirmed to be absent in ΔSt3 MEFs (Fig. 3 B).

As MTs are denatured during the preparation of total cell lysates (TCLs), we next investigated the levels of tubulin polymers specifically by harvesting cells in a MT-stabilizing buffer and performing differential sedimentation of polymerized tubulin from free tubulin. These results indicated that the amount of α-tubulin polymers in the pellet fraction of ΔSt3 MEFs was substantially reduced with a concomitant increase of free α-tubulin in the soluble fraction when compared with WT cells (Fig. 3 C, top). Similarly, the amount of acetylated α-tubulin polymers in ΔSt3 MEF cells was reduced (Fig. 3 C, second panel). Reprobing with an antibody for GAPDH indicated equivalent protein loading between samples (Fig. 3 C, third panel). Densitometric analysis indicated similar total levels of tubulin (i.e., soluble and pellet fractions combined) between the MEF cells (not depicted). In addition, Stat3 in WT MEFs was predominantly located in the soluble fraction and did not pellet down with MTs (Fig. 3 C, fourth panel), suggesting that Stat3 is not directly associated with MTs in vivo. To confirm the specificity of this method, we pretreated WT MEFs with taxol or nocodazole before harvesting. As shown in Fig. 3 C (bottom), the majority of α-tubulin in taxol-pretreated cells was found in the pellet. Conversely, no α-tubulin was found in the pellet of nocodazole-pretreated cells. This confirms the polymerized state of tubulin found in the pellet fractions.

To exclude the possibility that the differences in tubulin polymer content was caused by a change in cell cycle state in the ΔSt3 cells, we measured the DNA content of ΔSt3 compared with WT MEFs by propidium iodide staining and cell sorting. The percentages of cells in the various cell cycle states did not differ markedly between the two cell types (Fig. 3 D). Finally, as MTs influence cell motility, we assessed ΔSt3 MEF cell migration and demonstrated a severely reduced capacity to migrate into an in vitro wound track (Fig. 3 E). This is in agreement with previous reports of Stat3 function in regulating cell motility (Sano et al., 1999). Collectively, our data demonstrate that Stat3 ablation in MEF cells results in a perturbed MT network and impaired cell migration.

Stat3 expression promotes MT formation

To determine whether Stat3 expression could promote MT formation, we reintroduced Stat3 into ΔSt3 MEFs by retroviral infection. Reexpression of Stat3 restored the level of acetylated MTs in ΔSt3 MEFs to a level comparable with WT cells (Fig. 4 A). In addition, the amount of polymerized α-tubulin in retrovirally infected ΔSt3 MEFs was elevated above that of uninfected cells (or ΔSt3 MEFs infected with retrovirus vector) and was comparable with that in WT MEFs (Fig. 4 B). Reprobing for Stat3 confirmed reexpression in cells infected with Stat3 retrovirus only, and reprobing for GAPDH demonstrated equivalent protein loading.

To further characterize Stat3 regulation of MT stability in other cell types, endogenous Stat3 was down-regulated in

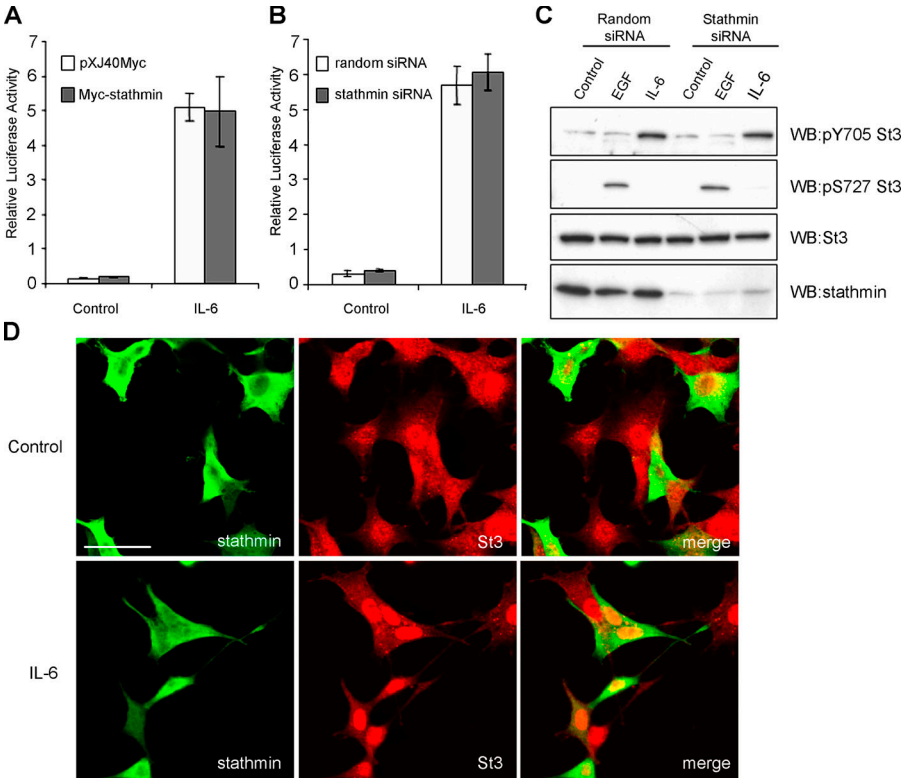

Figure 2. **Effect of stathmin on Stat3 signaling.** (A) PC12 cells were transfected with myc-tagged stathmin or a vector control (pXJ40-myc) along with the m67luc construct for a reporter gene assay to measure Stat3 transcriptional activity. Relative luciferase activity was measured after 8 h of stimulation with IL-6. Control samples in all of the panels were left unstimulated. (B) PC12 cells expressing stathmin siRNA or a vector encoding a random sequence were measured for IL-6–stimulated Stat3 luciferase activity as described in A. Error bars represent SEM. (C) PC12 cells expressing stathmin siRNA or a random vector control were stimulated with 100 ng/ml EGF or 40 ng/ml IL-6 for 15 min. Stat3 Y705 and S727 phosphorylation was then analyzed by immunoblotting. Reprobing for total Stat3 protein levels served as a control for loading. Blotting lysates with anti-stathmin showed the extent of stathmin down-regulation. (D) PC12 cells expressing myc-tagged stathmin were stimulated with 40 ng/ml IL-6 for 15 min or left unstimulated as a control. Stathmin and Stat3 localization was then determined by indirect immunofluorescence. Images are shown individually or merged. Bar, 20 μm.

MCF-7 cells by transient expression of a human Stat3 siRNA sequence. As a control, transfection with the empty siRNA vector did not affect Stat3 expression or acetylated MTs (Fig. 4 C, i–iii). In contrast, MCF-7 cells with reduced Stat3 expression exhibited a decrease in the amount of acetylated MTs (Fig. 4 C, iv–vi; arrows). Finally, we demonstrated that the expression in ΔSt3 MEFs of WT Stat3 or a Stat3 mutant (Y705F) previously shown to be deficient in transcriptional activity (Kaptein et al., 1996) induced a normal MT network morphology as detected by antibodies against α-tubulin (Fig. 4 D) and acetylated α-tubulin (Fig. 4 E). In contrast, a transcriptionally active Stat3 mutant (Stat3C; Bromberg et al., 1999) did not markedly rescue the MT network in these cells (Fig. 4, D and E). This suggests that the effect of Stat3 on MTs may be independent of the transcriptional activity of the dimer. In support of this, we also found that ligand-induced activation of Stat3, as indicated by Y705 or S727 phosphorylation, had little effect on the polymerized MT mass in WT MEFs (Fig. S1 A, available at http://www.jcb.org/cgi/content/full/jcb.200503021/DC1). Likewise, complete disruption of the MT network did not perturb ligand-stimulated Stat3 tyrosine phosphorylation (Fig. S1 B). In total, these results indicate that the cytosolic expression of Stat3 promotes MT formation, which may be independent of its nuclear activity.

Stat3 attenuates MT depolymerization induced by stathmin in MEFs

We next sought to identify the specific mechanism through which Stat3 regulated MT assembly. We could not find a direct association between Stat3 and either α- or β-tubulin in WT MEFs (Fig. S2 A, available at http://www.jcb.org/cgi/content/full/jcb.200503021/DC1). In addition, the MT network was not required for Stat3–stathmin interaction, as nocodazole pretreatment did not prevent coimmunoprecipitation of stathmin with Stat3 (Fig. S2 B). We next investigated whether the Stat3–stathmin interaction was involved in modulating MTs. We first determined the region of stathmin that was required for Stat3 interaction by deleting various amino acids from the NH_2 or COOH terminus of stathmin (Fig. 5 A). These mutants were then expressed in WT MEFs, and their interaction with endogenous Stat3 was analyzed. Stathmin deletion mutants truncated from the COOH terminus (aa 1–120 and 1–90) displayed a marked reduction in association with Stat3 in comparison with full-length or NH_2-terminally (aa 30–150 and 60–150) truncated stathmin (Fig. 5 B). This indicates that Stat3 binds to the COOH-terminal region of stathmin, which is also involved in binding tubulin. Surprisingly, although Stat3 bound to the full-length SCLIP, its binding capacity to the SLD of SCLIP (SCLIP-SLD, aa 38–180) was significantly reduced (Fig. 5 C). This suggests that the NH_2 terminus of SCLIP may be also required for Stat3 binding. However, because of the loss of membrane-anchoring cysteine residues, it remains unclear whether Golgi localization or the intrinsic presence of the SCLIP NH_2 terminus is required for the Stat3 association.

We next investigated Stat3 contribution to MT depolymerization induced by stathmin overexpression in WT compared with ΔSt3 MEFs. In addition, given the differences in Stat3 binding, the effect of SCLIP-SLD overexpression was simultaneously assessed for comparison. We found that the MT network remained largely intact in WT MEFs overexpressing stathmin (Fig. 5 D, i–iii). This is in agreement with the previously reported effects of stathmin overexpression on the MT network of *Xenopus laevis* A6 endothelial cells (Niethammer et al., 2004).

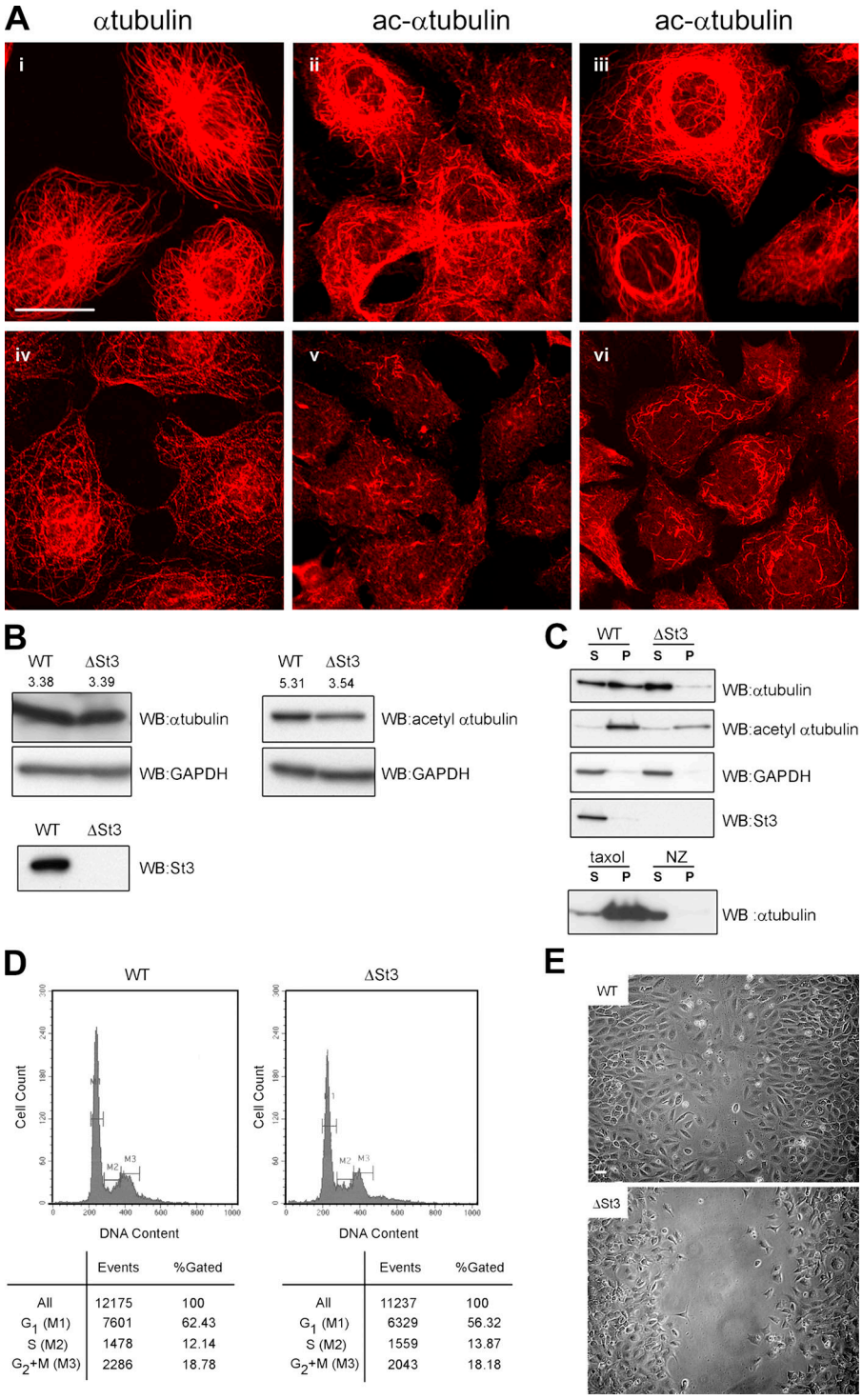

Figure 3. **MTs are disrupted in ΔSt3 MEF cells.** (A) WT (i–iii) and ΔSt3 (iv–vi) MEF cells were fixed and stained for α-tubulin or acetylated α-tubulin as indicated. Cells were also treated with 2 μM HU for 24 h before staining for acetylated α-tubulin (iii and vi). Bar, 20 μm. (B) Whole cell lysates from WT and ΔSt3 MEF cells were probed with the indicated antibodies. (C) Polymerized tubulin (P) was differentially sedimented from soluble tubulin (S) in WT and ΔSt3 lysates prepared in a MT-stabilizing buffer. Soluble and polymerized tubulin fractions were then analyzed by blotting for α-tubulin and acetylated α-tubulin. Membranes were then reprobed for Stat3 and GAPDH. Tubulin fractions were also differentially extracted from WT MEFs pretreated with 10 μM taxol (4 h) or 10 μM nocodazole (NZ; 4 h) and blotted for α-tubulin. (D) WT and ΔSt3 MEFs were stained with 50 μg/ml propidium iodide for cell cycle analysis by flow cytometry. M1 corresponds to cells in G_1, M2 to cells in S phase, and M3 corresponds to G_2/M phase. (E) WT and ΔSt3 MEF cells were seeded at confluency and subjected to scratch wounding. Wound closure was evaluated and recorded after 24 h.

However, the reduced MT network in ΔSt3 MEFs was further depolymerized by stathmin in ΔSt3 cells as indicated by the dispersed punctate α-tubulin staining in the positively transfected cell (Fig. 5 D, iv–vi). This different effect of stathmin is more clearly displayed in the enlarged images (Fig. 5 D, compare xiii with xiv). In contrast to stathmin, we observed that regardless of Stat3 expression, both WT and ΔSt3 MEFs overexpressing SCLIP-SLD showed certain degrees of MT depolymerization (Fig. 5 D, vii–xii). The different behavior of stathmin and SCLIP-SLD was not caused by the different expression level because their expression was comparable in both WT and ΔSt3 MEF cells (Fig. 5 E). These results suggest that endogenous Stat3 may prevent MT disassembly induced by stathmin but not SCLIP-SLD overexpression via a functional interaction.

A key factor in a mechanism where Stat3 promotes MT formation through an antagonistic interaction with stathmin is the presence of sufficient Stat3 protein in relation to stathmin. Therefore, we determined the absolute intracellular levels of

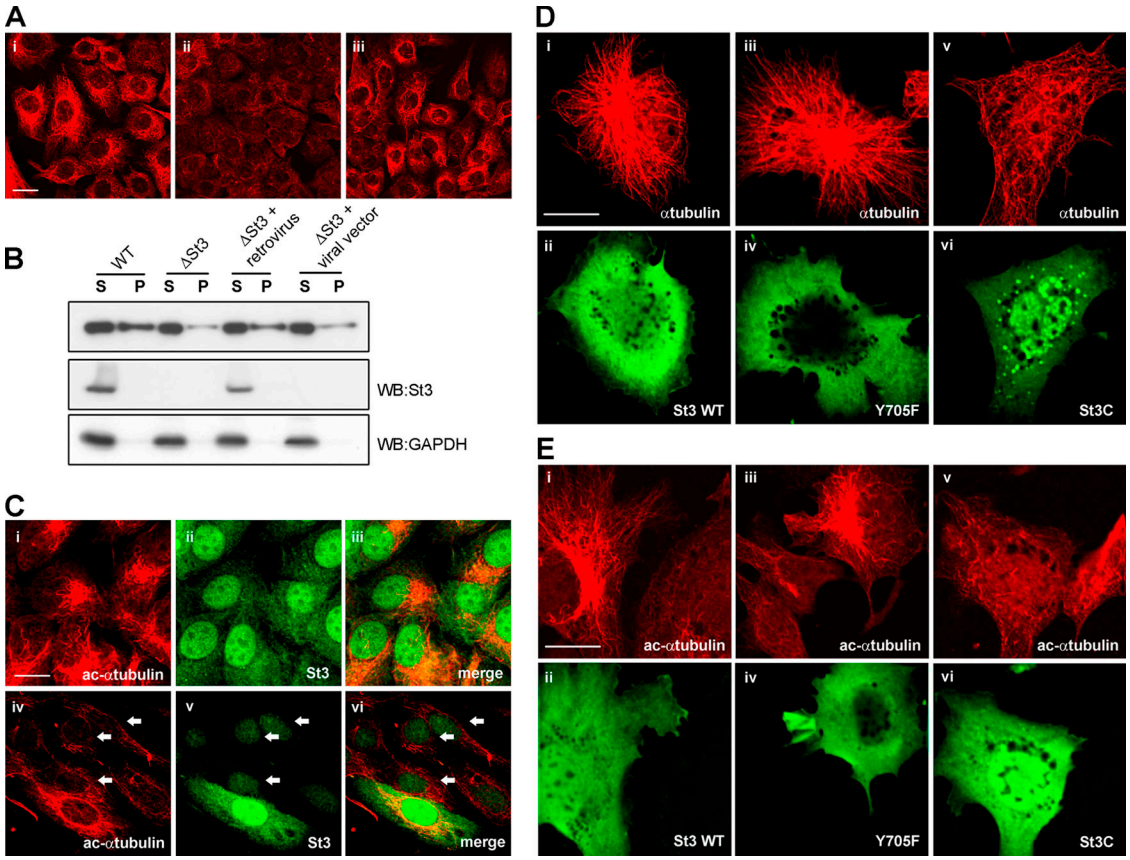

Figure 4. **Stat3 promotes MT formation.** (A) WT (i), ΔSt3 (ii), and ΔSt3 MEF cells infected with a retrovirus expressing Stat3 (iii) were stained for acetylated α-tubulin. (B) ΔSt3 MEF cells were infected either with a retrovirus expressing Stat3 (ΔSt3 + retrovirus) or an empty control vector (ΔSt3 + viral vector). Polymerized (P) and soluble (S) α-tubulin was then differentially extracted and analyzed by blotting. Stat3 expression was also confirmed by immunoblotting. Blots were reprobed for GAPDH as a loading control. WT and uninfected ΔSt3 MEFs were analyzed simultaneously for comparison. (C) MCF-7 cells were transfected with a vector expressing human Stat3 siRNA (iv–vi) or an empty control vector (i–iii). Cells were then fixed and stained for acetylated α-tubulin and Stat3. Arrows indicate cells with down-regulated expression of Stat3. (D and E) ΔSt3 MEF cells were transiently transfected with Flag-tagged WT Stat3 (i and ii), point mutated Stat3 Y705F (iii and iv), or an active form of Stat3 (St3C; v and vi). Cells were then stained for Stat3 protein, and MTs were stained with anti–α-tubulin (D) or anti-acetylated α-tubulin (E). Bars, 20 μm.

Stat3 and stathmin protein in PC12 cells. There was roughly 2.5 times the number of cellular Stat3 to stathmin (Fig. S3, A–E; available at http://www.jcb.org/cgi/content/full/jcb.200503021/DC1). In MEFs, the estimated ratio of Stat3 versus stathmin was even higher (not depicted). These results indicate that intracellular Stat3 is present in sufficient amounts and is capable of preventing the disassembly of MTs induced by an interacting partner (stathmin) but not the noninteracting SCLIP-SLD protein.

Down-regulation of stathmin partially restores the impaired MT network and migration observed in ΔSt3 cells

Next, we down-regulated endogenous stathmin expression by siRNA to further investigate its contribution to disrupting MTs in ΔSt3 cells. We first demonstrated that stathmin knockdown did not overtly affect the level of polymerized α-tubulin in WT MEFs (Fig. 6 A). However, transient expression of increasing amounts of stathmin siRNA induced an increase in polymerized α-tubulin levels in ΔSt3 MEFs (Fig. 6 B). Densitometric quantitation indicated that in WT MEFs expressing control siRNA, polymerized α-tubulin in WT MEFs represented 61 ± 0.4% of total α-tubulin (Fig. 6 C). In contrast, polymerized tubulin was found to make up only 17 ± 3.8% of total tubulin in ΔSt3 MEFs expressing control siRNA. This increased to 39 ± 1.9% in ΔSt3 MEFs transfected with the highest amount of stathmin siRNA used, which was significantly elevated ($P < 0.005$), compared with cells expressing control siRNA (Fig. 6 C). As a control, the level of polymerized α-tubulin in WT MEF cells expressing similar amounts of stathmin siRNA was not markedly changed (57 ± 3.9% of total tubulin). These results indicate a contribution of stathmin to the loss of polymerized tubulin in ΔSt3 MEFs.

The contribution of stathmin activity to the migratory properties of MEFs was then examined. First, we showed that the expression of stathmin siRNA had no apparent effect on the ability of WT MEFs to migrate into a wound track (Fig. 6 D, i–iii). This correlated with the lack of effect of the stathmin siRNA on MT levels in the normal fibroblast (Fig. 6 A). In contrast, the deficiency in ΔSt3 MEF migration into a wound track was partially reversed by down-regulating stathmin (Fig. 6 D, iv–vi). Quantitative analysis indicated 30–70% ($P < 0.05$ and $P < 0.001$, respectively) restoration in migration into the wound track by ΔSt3 MEFs transfected with increasing concentrations of stathmin siRNA (Fig. 6 E). As an increased stathmin protein

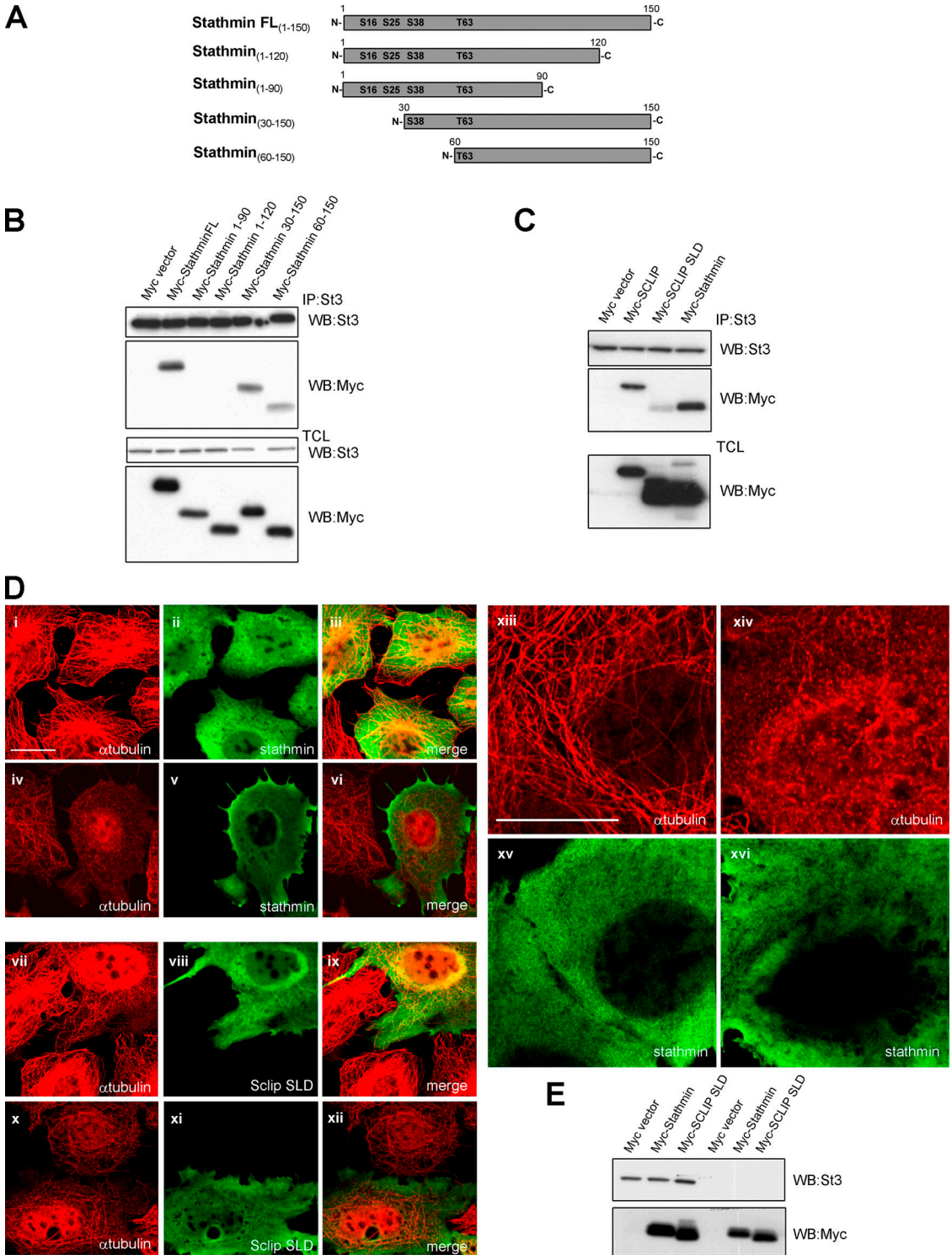

Figure 5. **Stat3 attenuates stathmin-induced MT depolymerization.** (A) Schematic representation of truncated mutants of stathmin. Conserved serine/threonine phosphorylation sites are also shown. (B) Myc-tagged stathmin mutants were transiently expressed in PC12 cells. Endogenous Stat3 was then immunoprecipitated, and the association of myc-tagged proteins was determined by immunoblotting. TCLs were also blotted for Stat3 and myc-tagged protein expression. (C) Coimmunoprecipitation of the myc-tagged full-length SCLIP, SCLIP-SLD, or stathmin with endogenous Stat3 was compared in WT MEF cells. (D) WT (i–iii, vii–ix, xiii, and xv) and ΔSt3 MEFs (iv–vi, x–xii, xiv, and xvi) were transiently transfected with either myc-tagged full-length stathmin (i–vi and xiii–xvi) or SCLIP-SLD (vii–xii). Cells were then fixed and stained with anti–α-tubulin and anti-myc. Bars, 20 μm. (E) The expression of myc-tagged stathmin and SCLIP-SLD in WT and ΔSt3 MEFs were determined by blotting.

expression had minimal effects on WT MEF cell migration (Fig. S4, available at http://www.jcb.org/cgi/content/full/jcb.200503021/DC1), these results suggest that excessive stathmin activity in a Stat3-null background is at least partially responsible for attenuating cell migration. In support of this, we observed that expression of a constitutively active mutant of stathmin

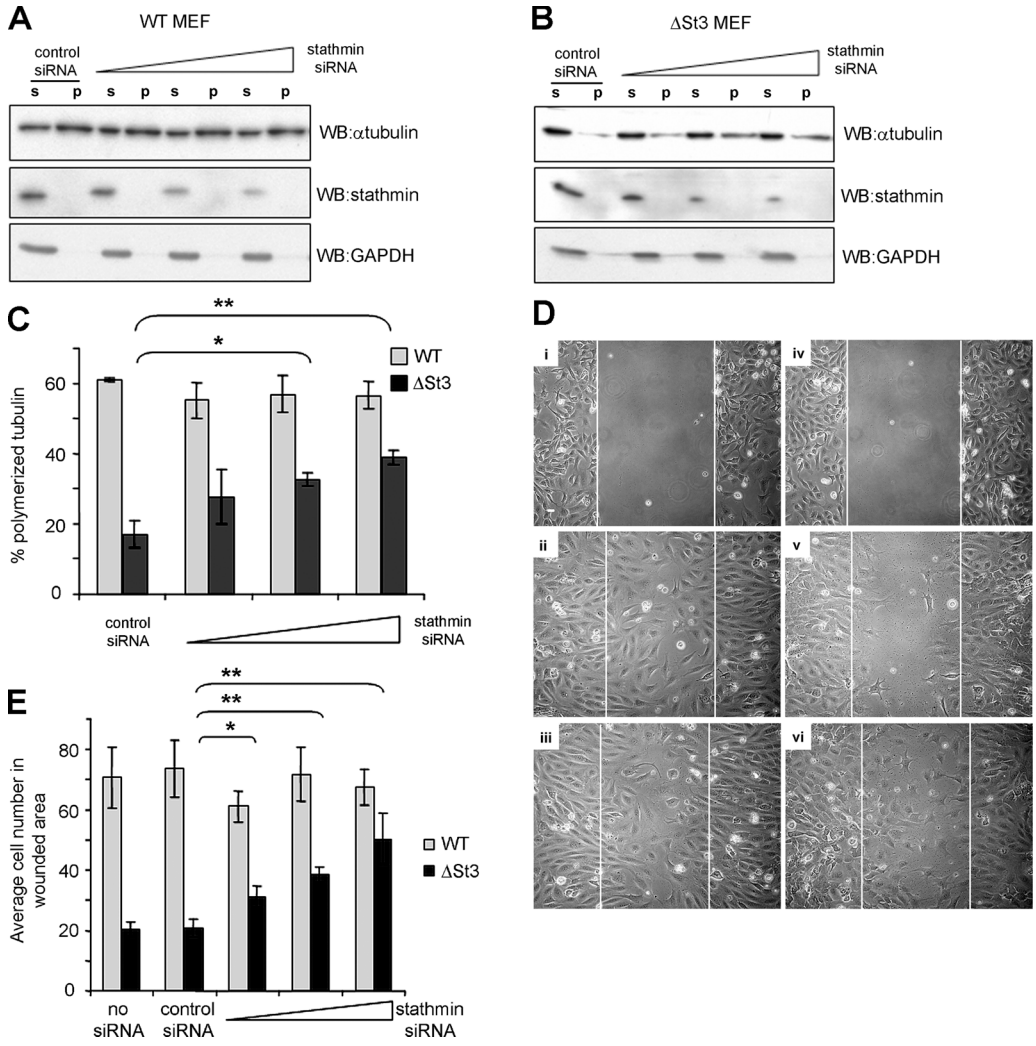

Figure 6. **Stathmin disassembly of MTs and attenuation of ΔSt3 MEF cell migration.** (A) WT and (B) ΔSt3 MEFs were transfected with increasing amounts of stathmin siRNA (0–30 nM), and the amount of α-tubulin in polymerized (p) and soluble (s) fractions was determined. Stathmin expression was also determined by Western blotting. Reprobing for GAPDH served as a protein loading control. (C) Tubulin bands were quantified by densitometric analysis, and polymerized tubulin was expressed as a percentage of total tubulin levels. *, $P < 0.05$; **, $P < 0.01$, as determined by paired *t* test analysis. (D) WT (i–iii) and ΔSt3 (iv–vi) MEFs expressing stathmin siRNA (30 nM; iii and vi) or a random sequence control (ii and v) were subjected to in vitro wounding before phase-contrast analysis after 24 h. The fields in between the white lines indicate the wound track. Bar, 20 μm. (E) The number of cells in the wound track from 10 random separate fields were counted for each treatment and expressed as a mean ± SD (error bars). *, $P < 0.0005$; **, $P < 0.001$, as determined by a paired *t* test.

(tetraA) prevented the migration of WT MEF cells into the wound track (Fig. S4). This correlated with the ability of stathmin tetraA to disassemble MTs in positively transfected WT MEF cells (not depicted). Altogether, our results point to stathmin as a possible downstream target of Stat3 in maintaining the MT array and normal cell migration.

Stat3 directly attenuates the MT-destabilizing activity of stathmin in vitro

We next sought to confirm that Stat3 could directly attenuate stathmin activity by using recombinant proteins in an in vitro tubulin assembly assay. GST-Stat3, GST-stathmin, and GST–SCLIP-SLD were produced in *E. coli* and purified by binding to glutathione–Sepharose beads. GST-Stat3 was further purified by gel filtration, whereas stathmin and SCLIP-SLD was generated by removing the GST tag by proteolytic cleavage. The final recombinant proteins were resolved by SDS-PAGE and stained by Coomassie blue (Fig. 7 A).

First, we demonstrated the normal kinetics of MT assembly, which included an initial nucleation stage followed by rapid polymerization that reached steady-state equilibrium at a ΔOD_{340} of 0.2–0.25 within 60 min under standard conditions (Fig. 7 B, control). Although including Stat3 did not affect the normal reaction, in the presence of stathmin, tubulin polymerization was severely inhibited (Fig. 7 B) to a level similar to a negative control containing nocodazole (not depicted). In addition, the inhibitory effect of stathmin on tubulin assembly was demonstrated to be dose dependent (Fig. 7 C). Next, we investigated the effect of GST-Stat3 in reversing stathmin attenuated MT assembly using different molar ratios of GST-Stat3 versus stathmin. We first showed that as a control, GST alone did not inhibit the activity of stathmin (Fig. 7 B). Subsequently, we

observed that although relatively low levels of GST-Stat3 (1:30 ratio to stathmin) had little effect, GST-Stat3 in a 1:5 molar ratio to stathmin restored MT polymerization to the same maximal level in comparison with the control (Fig. 7 D). These results indicated that GST-Stat3 reversed stathmin inhibition of MT polymerization in a dose-dependent manner. However, it was noticed that the normal polymerization kinetics were not completely restored. In the presence of GST-Stat3 and stathmin (1:5), the time required to reach maximum polymerization was >70 min compared with <40 min in the presence of tubulin alone (Fig. 7 D, control). Because of the low expression levels of the recombinant protein, a greater amount of GST-Stat3 could not be used without altering the total reaction volume and, subsequently, normal MT assembly kinetics.

The antagonistic function of Stat3 was further demonstrated by adding GST-Stat3 at ~30 min after the commencement of polymerization in the presence of stathmin. Upon adding Stat3, a reversal of stathmin that inhibited MT polymerization was immediately evident (Fig. 7 E), indicating that Stat3 could attenuate the interaction between stathmin and tubulin. As a control, GST had no such effect (Fig. 7 E). Finally, we showed that SCLIP-SLD, which does not interact with Stat3, can also inhibit MT assembly to a similar extent as stathmin but could not be attenuated when coincubated with GST-Stat3 (Fig. 7 F). These data demonstrate that Stat3 regulates the MT polymerization via direct interaction with stathmin. Indeed, in these MT polymerization reactions, GST-Stat3 directly interacted with stathmin, as shown by GST pull-down assays (Fig. 7 G).

To further address the effect of stathmin and Stat3, MTs were assembled using rhodamine-labeled tubulin, and the products were examined by fluorescence microscopy. In the control reaction, large amounts of long MT strands were formed after 30 min of incubation time (Fig. 7 H, i). In the presence of taxol, tubulin assembled into many short MT aggregates (Fig. 7 H, ii). This confirms the previously defined mechanism of taxol action in promoting MT assembly through stabilizing short tubulin polymers (Morejohn and Fosket, 1984). This indicates that, in vitro, taxol promotes a rapid absorbance increase in the turbiditometric assay through MT nucleation rather than elongation. As expected, incubating stathmin with tubulin prevented MT assembly, as shown by the lack of MTs after 30 min at 37°C (Fig. 7 H, iii) and the observation of only a few long MT strands after 60 min (Fig. 7 H, iv). However, preincubating stathmin with GST-Stat3 significantly rescued the assembly of MTs by 30 min, which improved further after 60 min (Fig. 7 H, v and vi). Furthermore, unlike taxol-assembled MTs, MT strands rescued by GST-Stat3 were long and comparable with untreated control MTs (Fig. 7 H, compare vi with i). These results, together with those shown in Fig. 7 E, indicate that stathmin inhibits the de novo formation of MTs. These results also clearly demonstrate a direct role for Stat3 in antagonizing the MT-destabilizing effect of stathmin to promote MT assembly.

Discussion

In this study, we identified the MT-destabilizing protein stathmin as a novel Stat3-interacting protein. To date, previously identified Stat3-interacting proteins have been concerned primarily with modulating Stat3 activity (Chung et al., 1997; Collum et al., 2000; Lufei et al., 2003). This does not appear to be the case with stathmin, as manipulating the expression of stathmin failed to perturb the phosphorylation, nuclear translocation, or transcriptional activity of Stat3 (Fig. 2). Instead, we present evidence that the association of Stat3 with stathmin may be involved in modulating the MT-destabilizing activity of the latter. Embryonic fibroblasts lacking Stat3 clearly exhibited a disrupted MT network with a lower level of polymerized and acetylated tubulin, which was reversed upon the reintroduction of Stat3 (Figs. 3 and 4). These results provide clear evidence that Stat3 is necessary for maintaining proper MT organization. However, there does not appear to be an obvious effect on mitotic MTs, as spindle formation and cell division do not appear perturbed in ΔSt3 MEFs (not depicted).

Stat3 had not been reported to directly associate with MTs. Our study supports this, as the pelleting of polymerized tubulin does not bring down Stat3 (Fig. 3 C). In addition, there was no obvious change in total tubulin protein (Fig. 3 B) or mRNA levels (not depicted) in ΔSt3 cells. This suggests that Stat3 does not directly modulate MT stability or tubulin expression. In contrast, our study indicates that Stat3 binds the COOH-terminal tubulin-binding domain of stathmin (Fig. 5), which is thought to contribute significantly, although not solely, to its MT-destabilizing activity (Curmi et al., 1997; Howell et al., 1999; Larsson et al. 1999). This suggests that Stat3 may compete for the tubulin-binding site to antagonize the MT-destabilizing activity of stathmin. In support of this, we show that recombinant Stat3 competitively binds and interferes with stathmin's activity in vitro (Fig. 7), implicating stathmin as a direct target of Stat3 in maintaining MT morphology. Furthermore, tubulin polymerization is reestablished in ΔSt3 cells by stathmin down-regulation (Fig. 6). In addition, stathmin overexpression disassembled MTs in ΔSt3 but not WT MEFs (Fig. 5). Although an increase in stathmin expression would be expected to result in MT disassembly in the normal cells, the extent of perturbation exerted on the MT array by exogenous stathmin depends largely on the level of expression achieved (Marklund et al., 1994; Niethammer et al., 2004). In contrast, we found that a similar expression level of SCLIP-SLD destabilized MTs irrespective of the presence of Stat3 in vivo (Fig. 5). This was further confirmed by the ability of recombinant Stat3 to attenuate the activity of stathmin, but not SCLIP-SLD, in vitro (Fig. 7 F). As the MT-destabilizing kinetics between these two highly homologous domains are similar in vitro (Fig. 7 F; Charbaut et al., 2001) and given their similar expression levels in vivo (Fig. 5 E), the main differentiating factor remains the expression of Stat3 in the MEF cells. However, as stathmin down-regulation only partially reversed the deficiency in MT levels and cell migration (Fig. 6), stathmin-independent mechanisms perturbed by the loss of Stat3 remains a possibility. Collectively, we conclude that a direct binding of stathmin by Stat3 serves to maintain the interphase MT array and support cell migration.

During the preparation of this manuscript, a similar study reported an interaction between stathmin and $p27^{Kip1}$, a cyclin-dependent kinase inhibitor protein (Baldassarre et al., 2005).

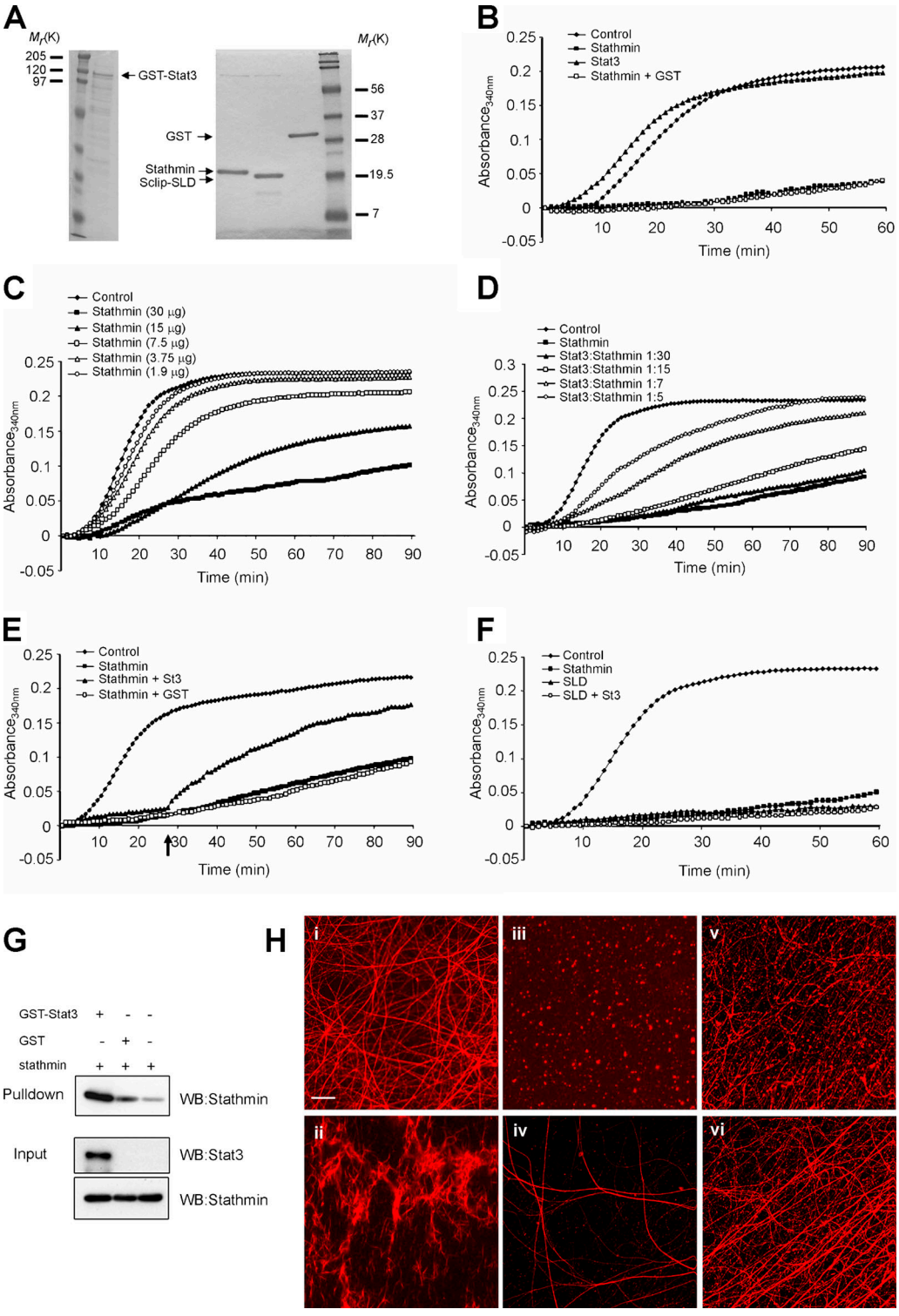

Figure 7. **Stat3 attenuates stathmin MT-destabilizing activity in vitro.** (A) Recombinant proteins (GST-Stat3, GST, stathmin, and SCLIP-SLD) used in the in vitro tubulin assembly experiments. (B) 300 μg tubulin was polymerized at 37°C in the presence of 35 μg GST-Stat3, 32 μg stathmin, 35 μg stathmin coincubated with GST, or an equivalent volume of buffer (control). (C) Tubulin was polymerized at 37°C in the presence of varying amounts of stathmin (1.9–30 μg). Polymerization in the presence of buffer alone was included as a positive control. (D) Tubulin was polymerized in the presence of 32 μg stathmin co-incubated with varying molar ratios of GST-Stat3 as indicated. Assembly in the presence of buffer or stathmin alone was included as positive and negative controls, respectively. (E) Tubulin assembly was conducted in the presence of 32 μg stathmin for 28 min (arrow). 35 μg GST-Stat3 or 35 μg GST was then added, and the reactions continued up to 90 min. Buffer or stathmin alone was included as a control. (F) Tubulin was assembled in the presence of 35 μg GST-Stat3, 32 μg stathmin, 32 μg SCLIP-SLD alone, or SCLIP-SLD coincubated with 35 μg GST-Stat3. (G) The interactions between stathmin and GST-Stat3 or GST in the in vitro MT polymerization assays were determined by GST pull-down. (H) 30 μg rhodamine-labeled tubulin was assembled at 37°C alone for 30 min (i), in the presence of 10 μM taxol for 30 min (ii), with 3.2 μg stathmin alone for 30 (iii) or 60 min (iv), or with stathmin preincubated with 3.5 μg GST-Stat3 for 30 (v) or 60 min (vi) and analyzed by fluorescence microscopy. Bar, 20 μm.

Although unclear, it remains possible that both proteins may be involved in regulating stathmin, depending on the cellular context. It is also interesting to note that $p27^{Kip1}$ expression is regulated by Stat3 (Klausen et al., 2000). In conjunction with this report, our current study supports the notion that the MT-destabilizing activity of stathmin may be regulated by protein–protein interaction in addition to serine/threonine phosphorylation. However, given that the nonphosphorylatable stathmin-tetraA constitutively active mutant could still disassemble MTs (not depicted) and halt migration in WT MEF cells (Fig. S4), serine phosphorylation clearly remains a key negative regulatory mechanism in stathmin function.

The loss of Stat3 severely affected the ability of MEFs to migrate into a wound track, which supports previous reports of Stat3 as a critical regulator of keratinocyte and ovarian cancer cell motility (Sano et al., 1999; Silver et al., 2004). As stathmin down-regulation promoted the migration of ΔSt3 MEFs (Fig. 6), inhibition of stathmin by Stat3 may, at least, be partially involved in maintaining cell motility in fibroblasts. We have also reported that the down-regulation of stathmin by siRNA in WT MEFs did not lead to a noticeable effect on MT polymer levels or cell migration (Fig. 6). Although the reason for this is unclear, we can postulate that the majority of stathmin in the interphasic cell may not be required for maintaining the MT array and may be kept inactive by negative regulatory mechanisms. In support of this was our observation that an increased expression of WT stathmin did not significantly perturb the MT array (Fig. 5) or migration (Fig. S4), suggesting that existing negative regulators of stathmin are sufficient for maintaining normal cell function. This is consistent with our observations that the wholesale loss of a negative regulator such as Stat3 would be detrimental to both the MT array and cell migration.

Some have made the reciprocal observation that an elevated expression of stathmin contributes to promoting cell migration (Baldassarre et al., 2005; Giampietro et al., 2005). However, this is counterintuitive to evidence that localized MT stabilization promotes cell migration through the establishment of cell polarity and preservation of the leading edge (Palazzo et al., 2004; Wen et al., 2004). Furthermore, a reduced level of stathmin–tubulin interaction has been described at the leading edge (Niethammer et al., 2004). In addition, a mild nocodazole treatment has also been shown to severely reduce fibroblast locomotion (Liao et al., 1995). Thus, excessive stathmin activity would likely be antimigratory. In confirmation of this, the expression of a constitutively active stathmin mutant prevented the migration of WT cells into the wound track (Fig. S4). However, although seemingly paradoxical, a chronic loss of stathmin activity, as is the case with stathmin-null fibroblasts (Baldassarre et al., 2005), may also be detrimental to cell migration as a result of a reduction in MT dynamics. In support of this, an analogous effect with taxol treatment also leads to a halt in cell motility (Liao et al., 1995). Thus, it appears that relative stathmin activity, as opposed to expression levels themselves, may be the more critical determinant in maintaining cell migration. Collectively, we propose that Stat3 regulation of stathmin activity is required to maintain MT dynamics to promote normal cell movement.

Stat3 function has traditionally been described in regard to its nuclear gene-regulating activity (for review see Bromberg and Darnell, 2000; Levy and Darnell, 2002). Although our results do not exclude a contribution by the transcriptional activity of Stat3, the notion that the Stat3–stathmin interaction is at least partially responsible for regulating MT assembly represents a key cytoplasmic function for Stat3. In support of this, fractionation studies have shown that after activation, an estimated 30% of Stats maximally and transiently accumulate in the nucleus (Carballo et al., 1999; Bienvenu et al., 2001) with a substantial amount of Stat3 remaining cytoplasmic. In addition, we have determined that intracellular Stat3, relative to stathmin, is present in sufficient amounts to antagonize the MT-destabilizing protein by direct interaction. Furthermore, the cytoplasmic expression of the Stat3 Y705F mutant was sufficient to promote the formation of acetylated MTs (Fig. 4). Given that perturbation of the MT network did not affect Stat3 activation (Fig. S1) and that stimulating Stat3 activity did not change MT polymer mass, the cytoplasmic and nuclear functions of Stat3 appear to be independent of one another.

In conclusion, our study has described a role for cytoplasmic Stat3 in mediating MT dynamics through functional interaction with a key MT-destabilizing protein, stathmin. MTs are central components of the cellular architecture required for proliferation, differentiation, and migration. Our work presents a novel mechanism through which Stat3 may mediate these processes in conjunction with its nuclear transcriptional activity.

Materials and methods

Yeast two-hybrid screening

$Stat3_{395–770}$ was cloned into the pGBKT7 plasmid containing the GAL4 DNA-binding domain and was used as bait in a yeast two-hybrid screen of a fetal mouse brain cDNA library (CLONTECH Laboratories, Inc.) as previously described (Lufei et al., 2003). After elimination of false positive clones by a β-gal colony lift-filter assay, plasmids were isolated from positive colonies, transformed into DH5α, purified, and sequenced.

Plasmid construction

Stathmin, SCG10, and SCLIP were amplified from a human fetal brain cDNA library (CLONTECH Laboratories, Inc.) by PCR with specific primers and subcloned into the pXJ40-myc vector with BamH1 and XhoI restriction enzymes. SCLIP-SLD and the truncated mutants of stathmin were subsequently generated by PCR, and the products were reinserted into pXJ40-myc. Stat3C was constructed from pRC-CMV-Stat3 by site-directed mutagenesis as previously described (Bromberg et al., 1999). All constructs were subjected to restriction digest and full sequencing analysis.

Recombinant protein purification

The GST-Stat3 fusion protein and the baculovirus-produced Stat3 were purified as previously described (Cao et al., 1996; Zhang et al., 2000). GST-Stat3 was further purified from cleavage products by fast protein liquid chromatography gel filtration through a Superdex HR200 column (GE Healthcare) equilibrated with 80 mM Pipes, pH 6.8, 1 mM EGTA, 5 mM $MgCl_2$, 10% (vol/vol) glycerol, and 1 mM benzamidine. The column was calibrated with the markers dextran blue (2,000 kD), femtin (440 kD), and cytochrome C (14 kD). Fractions corresponding to full-length GST-Stat3 were pooled and concentrated before use. The GST-stathmin and GST–SCLIP-SLD expression plasmid were constructed by inserting stathmin and SCLIP-SLD cDNA fragment into pGEX-6P-1 (GE Healthcare) vector with BamH1 and XhoI restriction enzymes. Plasmids were transfected to *E. coli*, and the expression of GST fusion proteins was induced with 100 mM IPTG for 4 h. GST fusion proteins were purified by binding to glutathione–Sepharose beads, eluted with 10 mM glutathione and 50 mM Tris-HCl, pH 8.0, and dialyzed into 80 mM Pipes, pH 6.8, 1 mM EGTA, 5 mM $MgCl_2$,

and 10% (vol/vol) glycerol. GST was then removed by Precision Protease cleavage according to optimized conditions (GE Healthcare).

Cell culture, drug treatments, and transfection

MCF7, NSC34, and MEFs were maintained in DME containing 10% FBS and supplemented with penicillin/streptomycin and L-glutamine. PC12 cells were similarly cultured but with an additional 5% (vol/vol) horse serum. MTs were polymerized by 10 μM taxol and depolymerized by 10 μM nocodazole for 4 h at 37°C before cell lysis. Transient transfections were performed with LipofectAMINE 2000 (Invitrogen) according to the manufacturer's instructions.

Immunofluorescence microscopy

Cells were grown on glass coverslips overnight to subconfluency. Subsequent to cell treatments, cells were fixed in 4% (wt/vol) PFA, permeabilized with 0.2% (vol/vol) Triton X-100 in PBS, and blocked with 10% (vol/vol) FCS in PBS. Cells were then stained with primary antibodies diluted (1:100) in 1% (wt/vol) BSA in PBS and detected withCy2/Cy3-conjugated secondary antibodies (1:400 in 0.1% [wt/vol] BSA in PBS). The cells were then mounted and examined on a confocal microscope (MRC1024; Bio-Rad Laboratories) using 40× NA 1.00 and 100× NA 1.25 oil immersion objectives (Carl Zeiss MicroImaging, Inc.) on an upright microscope (Axioplan2; Carl Zeiss MicroImaging, Inc.). Images were collected and processed using Lasersharp 2000 and Adobe Photoshop version 6.0, respectively.

Cell migration assay

Assay of cell migration into a wound area was performed as previously described (Sano et al., 1999) with slight modifications. In brief, WT and ΔSt3 MEF cells were grown to subconfluency on collagen (type I)-coated culture dishes (Iwaki). The cells were starved of serum for 24 h and treated with mitomycin C for 90 min to arrest cell proliferation. A wound track was then introduced by scraping the cell monolayer with a yellow pipette tip. Cells were cultured for a further 24–48 h before phase-contrast analysis.

siRNA

The siRNA expression vector containing a 21-nt target sequence for human Stat3 was constructed by insertion into pBS/U6 vector (a gift from Y. Shi, Harvard Medical School, Boston, MA) in two separate steps as previously described (Sui et al., 2002). The first annealed oligonucleotide pairs (5′-GGCGTCCATCCTGTGGTACAA-3′ and 5′-AGCTTTGTACCACAGGATGGACGCC-3′) were digested with ApaI (blunted) and HindIII. The inverted motifs that contained the six-nt spacer and five Ts (5′-AGCTTTGTACCACAGGATGGACGCCCTTTTTG-3′ and 5′-AATTCAAAAAGGGCGTCCATCCTGTGGTACAA-3′) were then subcloned into the intermediate plasmid (HindIII and EcoRI sites) to generate pBS/U6-hu Stat3 siRNA. A Basic Local Alignment Search Tool search of all target sequences showed no significant sequence homology with other genes. All siRNA expression vectors were confirmed by sequence analysis of the target insert. The murine stathmin synthetic siRNA (Santa Cruz Biotechnology, Inc.) was used according to the manufacturer's instructions.

In vivo polymerized tubulin assay

The in vivo assay of polymerized tubulin was performed as previously described (Minotti et al., 1991). In brief, MEF cells were scraped into a MT-stabilizing buffer (0.1 M Pipes, pH 6.9, 2 M glycerol, 5 mM $MgCl_2$, 2 mM EGTA, 0.5% Triton X-100, and protease inhibitors) supplemented with 4 μM taxol to maintain MT stability during isolation. The supernatant containing solubilized tubulin was clarified by centrifugation (20,000 *g* for 45 min) and separated from the pellet containing sedimented polymerized tubulin. The pellet was washed once in MT-stabilizing buffer before being denatured in laemmli buffer.

In vitro tubulin polymerization

The in vitro kinetics of MT assembly was measured using the Tubulin Polymerization Assay kit (Cytoskeleton, Inc.) according to the manufacturer's instructions. In brief, the assembly of 300 μg tubulin in 100 μl tubulin assembly buffer (80 mM Pipes, pH 6.8, 0.5 mM EGTA, 2 mM $MgCl_2$, 1 mM GTP, and 10% vol/vol glycerol) into MTs was started by incubating at 37°C. Absorbance at 340 nm was then measured every minute for up to 90 min in a temperature-controlled 96-well microtitre plate spectrophotometer (Genios; Tecan). Unless otherwise stated, recombinant proteins were coincubated for 10 min before the addition to tubulin. For fluorescence studies, 2 μg/μl tubulin was polymerized with rhodamine-labeled tubulin in a 4:1 ratio at 37°C for 30 or 60 min. MTs were then immediately spotted on a glass slide, an equal volume of Gel Mount (Biomeda) was added, and a coverslip was mounted. Images were then collected on a confocal microscope (MRC1024; Bio-Rad Laboratories) using a 100× NA 1.25 oil immersion objective (Carl Zeiss MicroImaging, Inc.) on an upright microscope (Axioplan2; Carl Zeiss MicroImaging, Inc.).

Online supplemental material

Fig. S1 shows that the MT polymerization state is independent of Stat3 activation. Fig. S2 shows that Stat3 does not associate with tubulin and that its binding to stathmin does not require the MT network. Fig. S3 indicates the quantification of Stat3 and stathmin protein in PC12 cells, and Fig. S4 shows that constitutively active stathmin attenuates cell migration. Online supplemental material is available at http://www.jcb.org/cgi/content/full/jcb.200503021/DC1.

We thank M. Gullberg for providing pMEP-stathmin tetraA, Y. Shi for pBS/U6, and G.P. Nolan for the Phoenix-Eco packaging cell line.

This work was supported by the Agency for Science, Technology, and Research of Singapore. X. Cao is an adjunct staff in the Department of Biochemistry at the National University of Singapore.

Submitted: 4 March 2005
Accepted: 13 December 2005

References

Akira, S. 2000. Roles of STAT3 defined by tissue-specific gene targeting. *Oncogene*. 19:2607–2611.

Baldassarre, G., B. Belletti, M.S. Nicoloso, M. Schiappacassi, A. Vecchione, P. Spessotto, A. Morrione, V. Canzonieri, and A. Colombatti. 2005. $p27^{Kip1}$-stathmin interaction influences sarcoma cell migration and invasion. *Cancer Cell*. 7:51–63.

Belmont, L.D., and T.J. Mitchison. 1996. Identification of a protein that interacts with tubulin dimers and increases the catastrophe rate of microtubules. *Cell*. 84:623–631.

Bienvenu, F., H. Gascan, and O. Coqueret. 2001. Cyclin D1 represses STAT3 activation through a Cdk4-independent mechanism. *J. Biol. Chem.* 276:16840–16847.

Bowman, T., R. Garcia, J. Turkson, and R. Jove. 2000. STATs in oncogenesis. *Oncogene*. 19:2474–2488.

Bromberg, J. 2002. Stat proteins and oncogenesis. *J. Clin. Invest.* 109:1139–1142.

Bromberg, J., and J.E. Darnell Jr. 2000. The role of STATs in transcriptional control and their impact on cellular function. *Oncogene*. 19:2468–2473.

Bromberg, J.F., M.H. Wrzeszczynska, G. Devgan, Y. Zhao, R.G. Pestell, C. Albanese, and J.E. Jr. Darnell. 1999. Stat3 as an oncogene. *Cell*. 98:295–303.

Cao, X., A. Tay, G.R. Guy, and Y.H. Tan. 1996. Activation and association of Stat3 with Src in v-Src transformed cell lines. *Mol. Cell. Biol.* 16:1595–1603.

Carballo, M., M. Conde, R.E. Bekay, J. Martin-Nieto, M.J. Camacho, J. Monteseirin, J. Conde, F.J. Bedoya, and F. Sobrino. 1999. Oxidative stress triggers STAT3 tyrosine phosphorylation and nuclear translocation in human lymphocytes. *J. Biol. Chem.* 274:17580–17586.

Charbaut, E., P.A. Curmi, S. Ozon, S. Lachkar, V. Redeker, and A. Sobel. 2001. Stathmin family proteins display specific molecular and tubulin binding properties. *J. Biol. Chem.* 276:16146–16154.

Chung, C.D., J. Liao, B. Liu, X. Rao, P. Jay, P. Berta, and K. Shuai. 1997. Specific inhibition of Stat3 signal transduction by PIAS3. *Science*. 278:1803–1805.

Collum, R.G., S. Brutsaert, G. Lee, and C. Schindler. 2000. A Stat3-interacting protein (StIP1) regulates cytokine signal transduction. *Proc. Natl. Acad. Sci. USA*. 97:10120–10125.

Costa-Pereira, A.P., S. Tininini, B. Strobl, T. Alonzi, J.F. Schlaak, H. Is'harc, I. Gesualdo, S.J. Newman, I.M. Kerr, and V. Poli. 2002. Mutational switch of an IL-6 response to an interferon-γ-like response. *Proc. Natl. Acad. Sci. USA*. 99:8043–8047.

Curmi, P., S.S. Andersen, S. Lachkar, O. Gavet, E. Karsenti, M. Knossow, and A. Sobel. 1997. The stathmin/tubulin interaction in vitro. *J. Biol. Chem.* 272:25029–25036.

Darnell, J.E., Jr., I.M. Kerr, and G.R. Stark. 1994. Jak-Stat pathways and transcriptional activation in response to IFNs and other extracellular signaling proteins. *Science*. 264:1415–1421.

Gavet, O., S. Ozon, V. Manceau, S. Lawler, P. Curmi, and A. Sobel. 1998. The stathmin phosphoprotein family: Intracellular localization and effects on the microtubule network. *J. Cell Sci.* 111:3333–3346.

Giampietro, C., F. Luzzati, G. Gamborotta, P. Giacobini, E. Boda, A. Fasolo, and I. Perroteau. 2005. Stathmin expression modulates migratory properties of GN-11 neurons in vitro. *Endocrinology*. 146:1825–1834.

Heim, M.H., I.M. Kerr, G.R. Stark, and J.E. Jr. Darnell. 1995. Contribution of STAT SH2 groups to specific interferon signaling by the Jak-STAT pathway. *Science*. 267:1347–1349.

Howell, B., N. Larsson, M. Gullberg, and L. Cassimeris. 1999. Dissociation of the tubulin-sequestering and microtubule catastrophe-promoting activities of oncoprotein 18/stathmin. *Mol. Biol. Cell*. 10:105–118.

Iancu, C., S.J. Mistry, S. Arkin, S. Wallenstein, and G.F. Atweh. 2001. Effect of stathmin inhibition on the mitotic spindle. *J. Cell Sci.* 114:909–916.

Kaptein, A., V. Paillard, and M. Saunders. 1996. Dominant negative Stat3 mutant inhibits interluekin-6-induced Jak-STAT signal transduction. *J. Biol. Chem.* 271:5961–5964.

Klausen, P., L. Pedersen, J. Jurlander, and H. Baumann. 2000. Oncostatin M and interleukin 6 inhibit cell cycle progression by prevention of p27kip1 degradation in HepG2 cells. *Oncogene*. 19:3675–3683.

Larsson, N., B. Segerman, B. Howell, K. Fridell, L. Cassimeris, and M. Gullberg. 1999. Op18/stathmin mediates multiple region-specific tubulin and microtubule-regulating activities. *J. Cell Biol.* 146:1289–1302.

Levy, D.E., and J.E. Darnell Jr. 2002. Stats: transcriptional control and biological impact. *Nat. Rev. Mol. Cell Biol.* 3:651–662.

Levy, D.E., and C.K. Lee. 2002. What does Stat3 do? *J. Clin. Invest.* 109:1143–1148.

Liao, G., T. Nagasaki, and G.G. Gundersen. 1995. Low concentrations of nocodazole interfere with fibroblast locomotion without significantly affecting microtubule level: implication for the role of dynamic microtubules in cell locomotion. *J. Cell Sci.* 108:3473–3483.

Lufei, C., J. Ma, G. Huang, T. Zhang, V. Novotny-Diermayr, C.T. Ong, and X. Cao. 2003. GRIM-19, a death-regulatory gene product, suppresses Stat3 activity via functional interaction. *EMBO J.* 22:1325–1335.

Marklund, U., O. Osterman, H. Melander, A. Bergh, and M. Gullberg. 1994. The phenotype of a "Cdc2 kinase target site-deficient" mutant of oncoprotein 18 reveals a role of this protein in cell cycle control. *J. Biol. Chem.* 269:30626–30635.

Minotti, A.M., S.B. Barlow, and F. Cabral. 1991. Resistance to antimitotic drugs in Chinese hamster ovary cells correlates with changes in the level of polymerized tubulin. *J. Biol. Chem.* 266:3987–3994.

Morejohn, L.C., and D.E. Fosket. 1984. Taxol-induced rose microtubule polymerization in vitro and its inhibition by colchicines. *J. Cell Biol.* 99:141–147.

Niethammer, P., P. Bastiaens, and E. Karsenti. 2004. Stathmin-tubulin interaction gradients in motile and mitotic cells. *Science*. 303:1862–1866.

Palazzo, A.F., C.H. Eng, D.D. Schlaepfer, E.E. Marcantonio, and G.G. Gundersen. 2004. Localized stabilization of microtubules by integrin- and FAK-facilitated Rho signaling. *Science*. 303:836–839.

Sano, S., S. Itami, K. Takeda, M. Tarutani, Y. Yamaguchi, H. Miura, K. Yoshikawa, S. Akira, and J. Takeda. 1999. Keratinocyte-specific ablation of Stat3 exhibits impaired skin remodeling, but does not affect skin morphogenesis. *EMBO J.* 18:4657–4668.

Silver, D.L., H. Naora, J. Liu, W. Cheng, and D.J. Montel. 2004. Activated signal transducer and activator of transcription (STAT) 3: Localization in focal adhesions and function in ovarian cell motility. *Cancer Res.* 64:3550–3558.

Sobel, A., M.C. Boutterin, L. Beretta, H. Chneiweiss, V. Doye, and H. Peyro-Saint-Paul. 1989. Intracellular substrates for extracellular signaling. Characterization of a ubiquitous, neuron-enriched phosphoprotein (stathmin). *J. Biol. Chem.* 264:3765–3772.

Sui, G., C. Soohoo, E.B. Affar, F. Gay, Y. Shi, W.C. Forrester, and Y. Shi. 2002. A DNA vector-based RNAi technology to suppress gene expression in mammalian cells. *Proc. Natl. Acad. Sci. USA*. 99:5515–5520.

Takeda, K., K. Noguchi, W. Shi, T. Tanaka, M. Matsumoto, N. Yoshida, T. Kishimoto, and S. Akira. 1997. Targeted disruption of the mouse Stat3 gene leads to early embryonic lethality. *Proc. Natl. Acad. Sci. USA*. 94:3801–3804.

Turkson, J., and R. Jove. 2000. STAT proteins: novel molecular targets for cancer drug discovery. *Oncogene*. 19:6613–6626.

Wang, T., G. Niu, M. Kortylewski, L. Burdelya, K. Shain, S. Zhang, R. Bhattacharya, D. Gabrilovich, R. Heller, D. Coppola, et al. 2004. Regulation of the innate and adaptive immune response by Stat-3 signaling in tumor cells. *Nat. Med.* 10:48–54.

Webster, D.R., and G.G. Borisy. 1989. Microtubules are acetylated in domains that turn over slowly. *J. Cell Sci.* 92:57–65.

Wei, D., X. Le, L. Wang, J.A. Frey, A.C. Gao, Z. Peng, S. Huang, H.Q. Xiong, J.L. Abbruzzese, and K. Xie. 2003. Stat3 activation regulates the expression of vascular endothelial growth factor and human pancreatic cancer angiogenesis and metastasis. *Oncogene*. 22:319–329.

Wen, Y., C.H. Eng, J. Schmoranzer, N. Cabrera-Poch, E.J. Morris, M. Chen, B.J. Wallar, A.S. Alberts, and G.G. Gundersen. 2004. EB1 and APC bind to mDia to stabilize microtubules downstream of Rho and promote cell migration. *Nat. Cell Biol.* 6:820–830.

Zhang, T., W.H. Kee, K.T. Seow, W. Fung, and X. Cao. 2000. The coiled-coil domain of Stat3 is essential for its SH2 domain-mediated receptor binding and subsequent activation induced by Epidermal Growth Factor and Interleukin-6. *Mol. Cell. Biol.* 20:7132–7139.